Journal Name

ARTICLE

Methylene-bridged Bimetallic Bis(imino)pyridine-Cobaltous Chlorides as Precatalysts for Vinyl-terminated Polyethylene Waxes

Received 00th January 20xx,
Accepted 00th January 20xx

DOI: 10.1039/x0xx00000x

www.rsc.org/

Qiang Chen,[a,b] Wenjuan Zhang,*[,a,c] Gregory A. Solan,*[,a,d] Tongling Liang,[a] Wen-Hua Sun*[,a,b]

Four examples of phenol-substituted methylene-bridged bis(imino)pyridines, CH(C_6H_4-4-OH){2'-(4-C_6H_2-2,6-R^2_2N=CMe)-6'-(2'',6''-$R^1_2C_6H_3$N=CMe)C_5H_3N}$_2$ [R^1 = R^2 = Me L1, R^1 = R^2 = Et L2, R^1 = Et, R^2 = Me L3, R^1 = ^{i}Pr, R^2 = Me L4], have been synthesized and fully characterized. Treatment of L1 – L4 with two equivalents of cobaltous chloride affords the bimetallic complexes, [(L)Co_2Cl_4] (L = L1 **Co1**, L2 **Co2**, L3 **Co3**, L4 **Co4**), in good yield. The molecular structure of **Co1** shows the two metal centers to be separated by a distance of 13.339 Å with each cobalt displaying a distorted trigonal bipyramidal geometry. On activation with either MAO or MMAO, **Co1** – **Co4** exhibited high activities for ethylene polymerization (up to 1.46 × 10^7 g(PE)·mol^{-1}(Co)·h^{-1} at 50 °C) with their relative values influenced by the steric properties of the N-aryl groups: **Co1** > **Co3** > **Co4** > **Co2**. Highly linear polyethylenes incorporating high degrees of vinyl end-groups are a feature of all the materials produced with the molecular weights of the MAO-promoted systems (M_w range = 2 - 8 kg mol^{-1}) generally higher than seen with MMAO (M_w range = 1 - 3 kg mol^{-1}), while the distributions using MMAO are narrower (PDI < 2.0).

Introduction

Late transition metal precatalysts that can be used to promote ethylene polymerization have attracted considerable attention due, in large measure, to their ease of preparation and to their capacity to generate a range of highly prized materials including highly linear polyethylene, waxes and highly branched polyethylenes. In particular, α-diimino-nickel(II) chlorides[1] and bis(imino)pyridine-iron(II) or -cobalt(II) chlorides[2] based on a single metal center, have been the subject of a wealth of reports since their first disclosure in the mid to late 1990's. Inspired by the synergistic role played by two closely located metal centers in enzymes such as that used for phosphate ester hydrolysis,[3] researchers have also been interested in applying similar concepts to the design of olefin polymerization catalysts. Indeed, this bio-inspired approach, in which the two polymerization-active metals are compartmentalized on the same multidentate ligand framework, has seen the development of catalysts that display activities and polyolefin microstructures that are not achievable *via* their mononuclear analogs.[4]

With regard to dinuclear cobalt systems, a range of pyridylimine-based supporting ligands have been developed including ones that incorporate inequivalent bi- and tri-dentate ligand pockets (**A** – **D**, Chart 1). In terms of catalytic performance, **A** showed moderate activity for ethylene oligomerization,[5] while **B** exhibited much higher activity and notably greater than its mononuclear analogs.[6] Similarly, dinuclear **C** exhibited very good activity (up to 1.7 × 10^7g·mol^{-1}·h^{-1}) for ethylene oligomerization with the major product being 1-butene.[7] By contrast, **D** showed much lower activity than **C** but produced a mixture of oligomer and polymer.[8]

Bimetallic cobalt precatalysts based on linked bis(imino)-pyridines such as **E** – **G** have also been the source of a number of reports (Chart 1). Indeed, all these complexes, containing apparently equivalent binding domains, display moderate to good activity for ethylene polymerization and, what is more, higher activity than that observed for their monomeric analogues. For example, **E** can reach activities as high as 2.4 × 10^7 g(PE)·mol^{-1}·h^{-1}, which is significantly greater than that reported for the corresponding mononuclear bis(imino)-pyridine-cobalt precatalyst.[9] In addition, biphenyl-bridged bis(imino)pyridine-cobalt chloride **F**, exhibited four times higher activity than its monomeric counterparts producing highly linear polyethylene. Moreover, these systems showed better thermal stability by operating efficiently at 50 °C.[10] Elsewhere, Takeuchi's group has reported the 'double-decker' binuclear cobalt species **G** which, though displaying only moderate activity, generated polyethylene with molecular weight much higher than its mononuclear comparators. Justification for this molecular weight enhancement was given

[a] *Key Laboratory of Engineering Plastics and Beijing National Laboratory for Molecular Sciences, Institute of Chemistry, Chinese Academy of Sciences, Beijing 100190, China. E-mail: whsun@iccas.ac.cn*
[b] *CAS Research/Education Center for Excellence in Molecular Sciences, University of Chinese Academy of Sciences, Beijing 100049, China.*
[c] *School of Materials Science and Engineering, Beijing Institute of Fashion Technology, Beijing 100029, China. E-mail: zhangwj@bift.edu.cn*
[d] *Department of Chemistry, University of Leicester, University Road, Leicester LE1 7RH, UK. E-mail: gas8@le.ac.uk.*
†CCDC 1828025 for **Co1**. For crystallographic data in CIF or other electronic format see DOI: 10.1039/XXXXX. Electronic Supplementary Information (ESI) available: [details of any supplementary

in terms of a cooperative interaction between the growing polymer and the second metal center that efficiently retarded undesirable deactivation of the catalyst and/or chain transfer.[11] Nevertheless, cooperative effects of this type remain scarce in cobalt chemistry and hence there is a drive to broaden the range of bimetallic cobalt polymerization catalysts so as to further probe such effects.[12]

In this work we target the phenol-substituted methylene-bridged bis(imino)pyridine-dicobalt chlorides **H** (Chart 1) with a view to assessing their performance as ethylene polymerization precatalysts. The role of steric factors imparted by the ligand frame will be investigated as will the nature of the co-catalyst and the temperature of the polymerization run. In addition, full synthetic and characterization data is presented for both the ligands and their corresponding complexes.

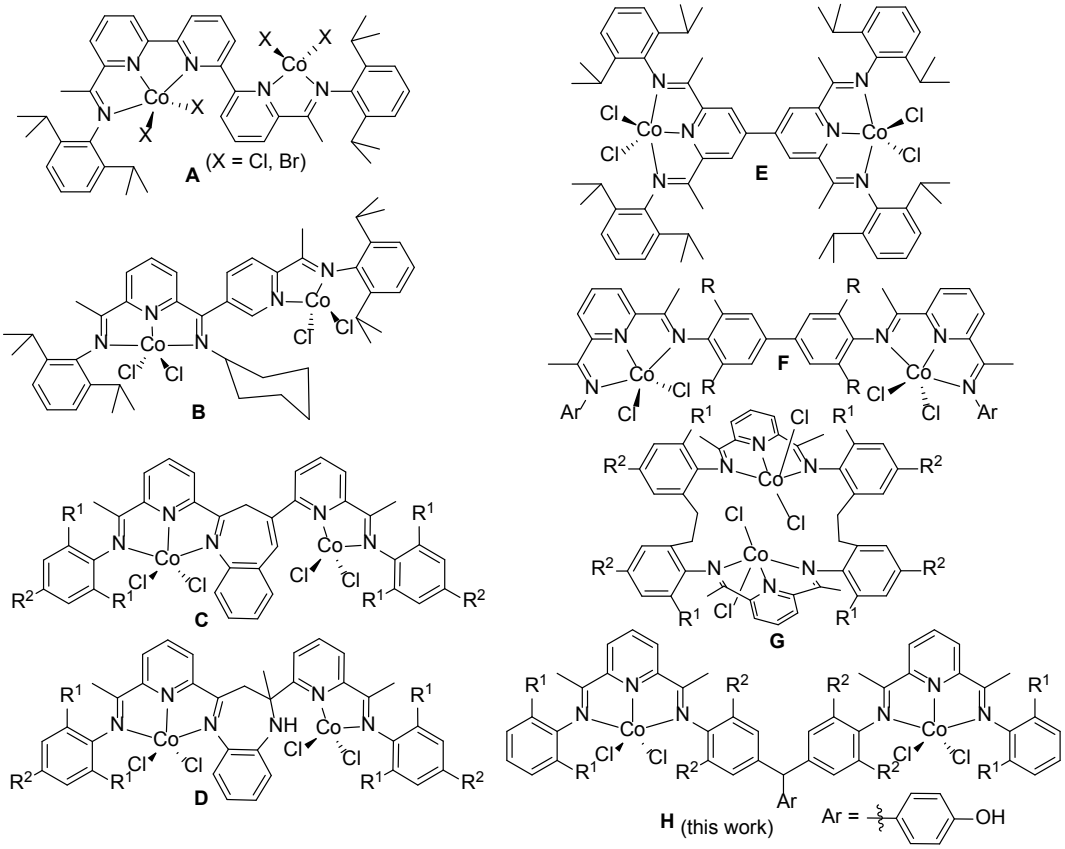

Chart 1 Previously reported dinuclear cobalt precatalysts, **A – G**, and target **H**.

Results and discussion

Synthesis of L1 – L4 and Co1 – Co4

The phenol-substituted methylene-bridged bis(imino)pyridines, CH(C_6H_4-4-OH){2'-(4-C_6H_2-2,6-R^2_2N=CMe)-6'-(2'',6''-$R^1_2C_6H_3$N=CMe)C_5H_3N}$_2$ [R^1 = R^2 = Me L1, R^1 = R^2 = Et L2, R^1 = Et, R^2 = Me L3, R^1 = ^{i}Pr, R^2 = Me L4], have been prepared in moderate yields by treating the corresponding diamine, CH(C_6H_4-4-OH)(4-C_6H_2-2,6-R_2NH_2)$_2$ (R = Me, Et), with just over two equivalents of the appropriate 2-acetyl-6-aryliminopyridine, 2-(CMeO)-6-{(CMe=N(2,6-$R^1_2C_6H_3$)}C_5H_3N (R^1 = Me, Et, ^{i}Pr), in *o*-xylene at reflux (Scheme 1). The precursor diamines and 2-acetyl-6-aryliminopyridines are not commercially available and have been prepared using literature procedures.[13] All new organic compounds have been characterized by ^{1}H/^{13}C NMR and FT-IR spectroscopy as well as by elemental analysis. Reaction of L1 – L4 with two equivalents of $CoCl_2$ in dichloromethane at room temperature gave [(L)Co_2Cl_4] (L = L1 **Co1,** L2 **Co2,** L3 **Co3,** L4 **Co4**) in good yields, respectively (Scheme 1). Each complex has been characterized by FT-IR spectroscopy, elemental analysis and in the case of **Co1** by single crystal X-ray diffraction.

Crystals of **Co1** suitable for an X-ray determination were grown by slow diffusion of diethyl ether into a methanol solution containing the complex. A view of the structure is shown in Figure 1a; selected bond lengths and angles are tabulated in Table 1. The structure consists of two cobalt dichloride units that are bound within the two essentially planar tridentate *N,N,N*-pockets belonging to L1. The five-coordinate geometry at each metal center can be best described as distorted trigonal bipyramidal with the pyridine nitrogen atom and two chlorides defining the equatorial plane. For each metal, the N-aryl groups are inclined almost perpendicularly to the neighboring imine vectors with the dihedral angles being 85.26° and 89.10° for Co(1) and 84.93° and 87.69° for Co(2). Of the three Co-N bond distances to each metal center, that involving the central pyridine [2.025(4), 2.030(4) Å] is shorter than the Co-N_{imine} distances [range: 2.219(4) - 2.272(4) Å]. Indeed, these Co-N_{imine} lengths are comparable to those observed in one example of a

mononuclear bis(imino)pyridine-$CoCl_2$ (*ca.* 2.211 Å).[14] Due to the sp^3-hybridisation of the bridging CH(C_6H_4-4-OH) group, the dihedral angle between the two *N,N,N*-chelation planes (N1-N2-N3 and N4-N5-N6) is 53.48°, with the result that the cobalt centers are positioned 13.339 Å apart. Additionally, the presence of the OH functionality on the phenol unit leads to adjacent molecules of **Co1** assembling *via* O···HO hydrogen bonding (2.706 Å, see Figure 1b).

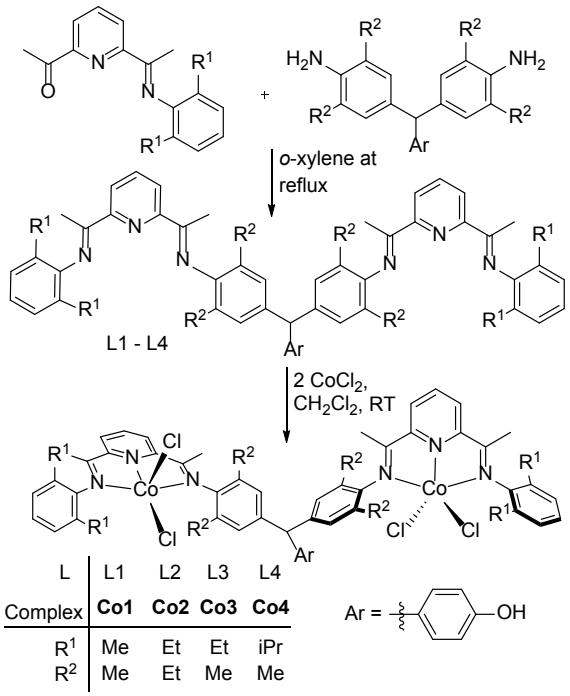

L	L1	L2	L3	L4
Complex	**Co1**	**Co2**	**Co3**	**Co4**
R^1	Me	Et	Et	iPr
R^2	Me	Et	Me	Me

Scheme 1 Synthesis of L1 – L4 and their binuclear complexes **Co1** – **Co4**

The microanalytical data for all four complexes are consistent with each adopting a composition based on [(L)Co_2Cl_4]. In their IR spectra the ν(C=N)$_{imine}$ stretching frequencies fall in the range 1617 - 1621 cm^{-1} which compares to 1639 - 1642 cm^{-1} for the free ligands, which provides further evidence that the metals are coordinated by the ligands.

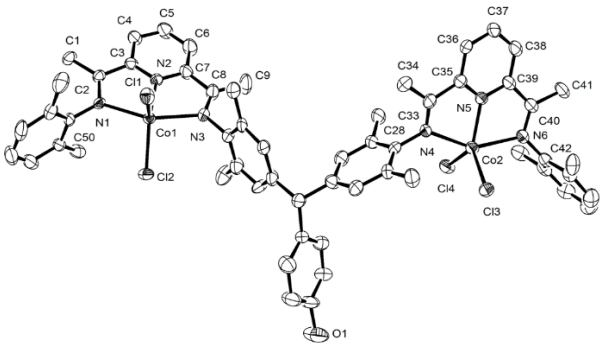

Fig. 1a ORTEP representation of **Co1**. The thermal ellipsoids are shown at the 30% probability level while the hydrogen atoms have been omitted for clarity.

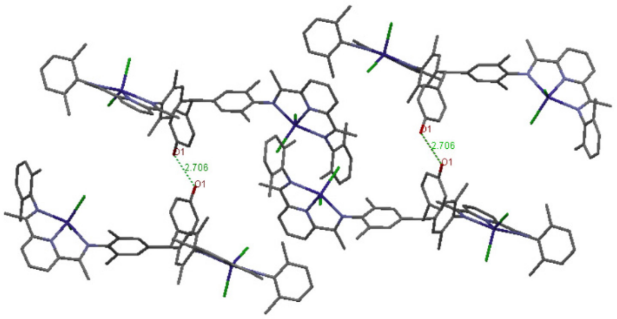

Fig. 1b O···HO hydrogen-bonding interactions between neighboring molecules of **Co1.**

Table 1 Selected bond lengths (Å) and angles (°) for **Co1**

Bond Lengths (Å)			
Co(1)-N(1)	2.219(4)	Co(2)-N(6)	2.261(4)
Co(1)-N(2)	2.025(4)	Co(2)-N(5)	2.030(4)
Co(1)-N(3)	2.272(4)	Co(2)-N(4)	2.272(4)
N(1)-C(2)	1.280(6)	N(6)-C(40)	1.278(6)
N(1)-C(50)	1.430(6)	N(6)-C(42)	1.440(7)
N(2)-C(3)	1.325(6)	N(5)-C(39)	1.348(6)
N(2)-C(7)	1.358(6)	N(5)-C(35)	1.353(7)
N(3)-C(10)	1.452(6)	N(4)-C(28)	1.414(6)
N(3)-C(8)	1.282(6)	N(4)-C(33)	1.287(7)
Bond Angles (°)			
N(2)-Co(1)-Cl(1)	107.90(13)	N(5)-Co(2)-Cl(4)	127.73(11)
N(3)-Co(1)-Cl(2)	96.24(11)	N(4)-Co(2)-Cl(3)	94.94(11)
N(1)-Co(1)-Cl(2)	100.75(10)	N(6)-Co(2)-Cl(3)	98.29(10)
Cl(2)-Co(1)-Cl(1)	117.46(6)	Cl(3)-Co(2)-Cl(4)	115.39(6)
C(3)-N(2)-C(7)	121.2(4)	C(39)-N(5)-C(35)	120.9(5)
C(2)-N(1)-C(50)	119.6(4)	C(40)-N(6)-C(42)	118.2(4)
C(8)-N(3)-C(10)	119.1(4)	C(33)-N(4)-C(28)	118.7(5)

Catalytic evaluation

Previous studies in iron- and cobalt-based ethylene polymerization have revealed that methylaluminoxane (MAO) or modified methylaluminoxane (MMAO) are generally more effective co-catalysts when compared with other alkyl-aluminum reagents.[15] Hence, these two aluminoxanes were independently employed in this study as co-catalysts to assess the performance of **Co1** – **Co4** as ethylene polymerization precatalysts.

(a) Ethylene polymerization using Co1 – Co4/MAO. Complex **Co1** was selected to optimize the polymerization parameters with MAO as co-catalyst; the results are collected in Table 2. In the first instance, the polymerization runs were conducted in toluene at various temperatures between 40 and 70 °C by fixing the Al/Co ratio at 1000 and the ethylene pressure at ten atmospheres. Inspection of the results show the highest polymerization activity of 5.73 × 10^6 g(PE)·mol^{-1}(Co)·h^{-1} was achieved at 50 °C (runs 1 - 4, Table 2). Raising the temperature further led to a lowering in activity which can be attributed to either decomposition of the active species or to the lower ethylene concentration in toluene at higher temperature.[15a,16] Nevertheless, even at 70 °C the activity still reached a good level of 2.35 × 10^6 g(PE)·mol^{-1}(Co)·h^{-1} which is notably higher than that seen by related mononuclear cobalt precatalysts

under comparable conditions,[2] indicating the improved thermal stability of the current system. At the same time the molecular weight of the polyethylene decreased from 7.7 to 4.0 kg mol^{-1} on increasing the temperature from 40 to 70 °C, which is consistent with faster chain transfer at higher temperature. Figure 2 depicts the GPC traces of the polyethylene produced by **Co1**/MAO at different temperatures which not only shows a gradual lowering of the molecular weight with temperature, but also highlights the essentially monomodal distribution of the polymers albeit with some shouldering (PDI 3.0 – 5.7).

Table 2 Ethylene polymerization results by **Co1** – **Co4**/MAO[a]

Run	Precat.	Al/Co	T/ °C	t/min	Polymer/g	Activity[b]	M_w[c]	M_w/M_n[d]	T_m[e]/ °C
1	**Co1**	1000	40	30	4.84	2.99	7.7	5.7	125.5
2	**Co1**	1000	50	30	8.59	5.73	6.7	4.9	125.6
3	**Co1**	1000	60	30	6.40	4.27	6.0	4.4	124.2
4	**Co1**	1000	70	30	3.52	2.35	4.0	3.0	124.3
5	**Co1**	1500	50	30	9.26	6.17	2.9	2.6	122.7
6	**Co1**	2000	50	30	10.4	6.93	2.5	2.3	121.8
7	**Co1**	2250	50	30	13.3	8.89	2.3	2.2	121.5
8	**Co1**	2500	50	30	12.3	8.21	2.4	2.2	121.5
9	**Co1**	3000	50	30	10.9	7.25	2.3	2.2	122.2
10	**Co1**	2250	50	5	3.65	14.6	2.3	2.2	121.8
11	**Co1**	2250	50	15	6.81	9.08	2.4	2.2	121.6
12	**Co1**	2250	50	45	13.8	6.14	2.6	2.3	121.9
13	**Co1**	2250	50	60	14.0	4.66	3.0	2.6	122.7
14[f]	**Co1**	2250	50	30	0.28	0.19	1.8	2.1	119.8
15[g]	**Co1**	2250	50	30	5.49	3.66	2.5	2.4	122.4
16	**Co2**	2250	50	30	8.29	5.53	3.6	2.7	124.7
17	**Co3**	2250	50	30	11.8	7.89	4.5	3.0	125.8
18	**Co4**	2250	50	30	9.89	6.59	11.0	3.5	129.6

[a] Conditions: 1.5 µmol of cobalt precatalyst; 10 atm of ethylene; total volume of solvent 100 mL;

[b] Activity: 10^6 g(PE)·mol^{-1}(Co)·h^{-1};

[c] M_w: kg mol^{-1};

[d] M_w and M_w/M_n determined by GPC;

[e] Determined by DSC;

[f] 1 atm of ethylene;

[g] 5 atm of ethylene.

By fixing the reaction temperature at 50 °C, the effect of changing the quantity of MAO on the performance of **Co1** was also investigated by varying the Al/Co molar ratio between 1000 and 3000 (runs 2, 5-9, Table 2). At a ratio of 2250, the highest activity of 8.89 × 10^6 g(PE)·mol^{-1}(Co)·h^{-1} was achieved.

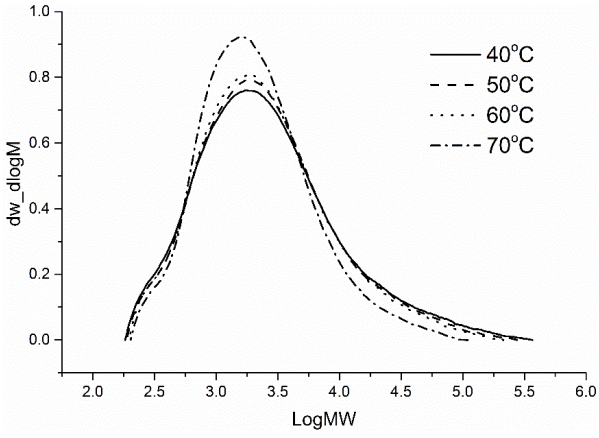

Fig. 2 GPC curves of the polyethylene generated using **Co1**/MAO at different temperatures (runs 1 – 4, Table 2)

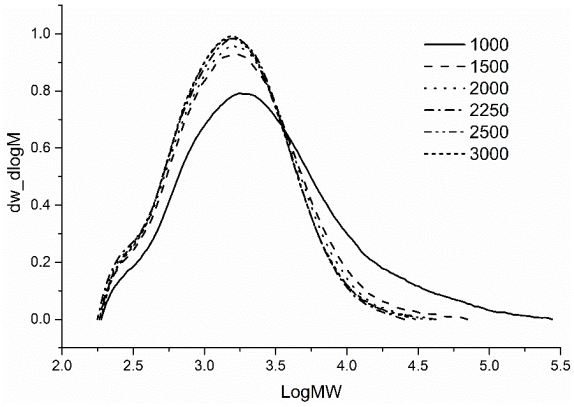

Fig. 3 GPC curves of the polyethylene produced using **Co1**/MAO at different molar ratio of Al/Co (runs 2, 5 – 9, Table 2)

Further increasing the Al/Co molar ratio to 3000 gradually decreased the activity from 8.89 to 7.25 × 10^6 g(PE)·mol^{-1}(Co)·h^{-1}. Furthermore, the molecular weight dramatically decreased from 6.7 to 2.9 kg mol^{-1} on altering the molar ratio

from 1000 to 1500. On the other hand, no significant change in the molecular weight was observed on further increasing the molar ratio to 3000 (M_w range: 2.3 to 2.9 kg mol^{-1}), an observation that is notably different to that seen in previous reports.[17] Indeed, the molecular weight usually dramatically decreases with higher amounts of MAO in line with increased chain transfer to the aluminum.[2a] These variations in molecular weight with Al/Co ratio are illustrated in the GPC curves (Figure 3); these curves once again show unimodal characteristics for the polymers with some shouldering a feature of each (PDI 2.2 - 4.9). It is tempting to ascribe this observation to some multi-site behavior of the catalyst.

To explore the effect of time on the performance of **Co1**/MAO, the polymerization runs were carried out at intervals between 5 and 60 minutes (run 7, 10 - 13, Table 2) with the temperature and Al/Co ratio kept at 50 °C and 2250, respectively. Over the course of the polymerization the activity gradually decreased from 14.6 (5 minutes) to 4.66 × 10^6 g(PE)·mol^{-1}(Co)·h^{-1} (60 minutes) in accord with some deactivation of the active species over prolonged reaction times;[18] a feature that is indeed common to many olefin polymerization catalysts.[2] Nonetheless, the polymerization activity after 60 minutes still remained relatively high at 4.66 × 10^6 g(PE)·mol^{-1}(Co)·h^{-1} (run 13, Table 2), highlighting the good catalytic lifetime of the active species when compared with related systems.[19] On decreasing the ethylene pressure from 10 to 1 atmospheres (runs 7, 14, 15, Table 2) with the temperature maintained at 50 °C and the Al/Co ratio at 2250, the polymerization activity sharply decreased from 8.89 to 0.19 × 10^6 g(PE)·mol^{-1}(Co)·h^{-1}. On the other hand, the molecular weight remained comparable (range: 1.8 - 2.3 kg mol^{-1}). This dependency of the activity on the pressure can be attributed to better ethylene coordination and in-turn activity at higher pressure.

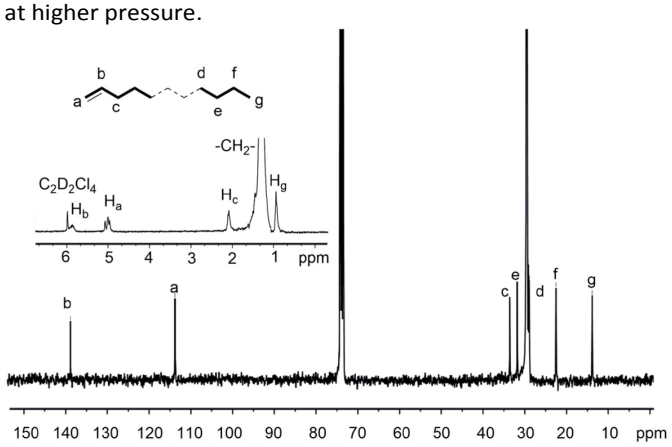

Fig. 4 ^{13}C NMR spectrum of the polyethylene obtained using **Co1**/MAO (run 7, Table 2) (recorded in tetrachloroethane-d_2: δC 73.8 ppm), along with an insert showing its ^{1}H NMR spectrum

With the optimized conditions established for **Co1**/MAO [Al/Co ratio at 2250, the temperature at 50 °C, ethylene pressure at 10 atmospheres and run time at 30 minutes], the performance of the remaining three cobalt complexes, **Co2** – **Co4** was investigated and compared with **Co1**. All precatalysts displayed good performance (5.53 - 8.89 × 10^6 g(PE)·mol^{-1}(Co)·h^{-1}) (runs 7, 16-18, Table 2) with the activity decreasing in the order: **Co1** (Me, Me) > **Co3** (Et, Me) > **Co4** (^{i}Pr, Me) > **Co2** (Et, Et). It would appear that the steric properties exerted by *ortho* R^1 and R^2 are both influential with increased hindrance leading to lower activity as a result of impeded ethylene coordination and insertion.[21] In terms of molecular weight, the polyethylene generated using **Co4** is much higher than that shown for **Co3**, **Co1** and **Co2** which lends support to the importance of the bulky ^{i}Pr (R^1) substituents on the external N-aryl group. It would seem likely that these hindered ^{i}Pr substituents (**Co4**) protect the active species and hence favor chain propagation leading to higher molecular weight polymer.[20] By way of comparison, these systems showed comparable activity to that observed with dicobalt complexes **E** and **F**.[9,10]

To probe the microstructural properties of the polyethylenes, the sample generated using **Co1**/MAO (run 7, Table 2) was characterized by ^{1}H/^{13}C NMR spectroscopy at high temperature (100 °C in 1,1,2,2-tetrachloroethane-d_2) (Figure 4). In the ^{1}H NMR spectrum, downfield multiplets at respectively δ 5.90 (H$_b$) and δ 5.05 (H$_a$) in a 1:2 ratio, are indicative of a vinyl-terminated polymer with the more upfield peaks corresponding to the CH$_2$ adjacent to the vinyl (H$_c$), the main CH$_2$ repeat unit and the methyl group (H$_g$) at the opposite end of the chain. Such signals are typical of a linear polymer which is corroborated by the 1:3 ratio of the vinylic H$_b$ to methyl H$_g$ protons. The ^{13}C NMR spectrum further confirms the vinyl-end functionality with characteristic signals at δ 111.4 and 139.5 along with signals for the saturated chain end (C$_d$, C$_e$, C$_f$ and C$_g$) (Figure 4).[22] Similar chain-ends were a feature of other polyethylenes formed with MAO as co-catalyst in this study; the corresponding NMR spectra for the polymer formed in run 2 (Table 2) are given in the supplementary information (Figure S1). Collectively, these findings suggest that these MAO-promoted polymerizations have a preference for a termination mechanism involving β-H transfer to metal or to the monomer,[14] rather than the sometimes observed transfer to aluminum.[2] Further support for the linearity of the polymers is provided by the typically high melting temperatures (T_m) for all the materials obtained in this particular study (Table 2). It is worthy of note that vinyl-terminated polymers of type produced here have some interest for use as monomers in the synthesis of functional polyethylenes.[23]

(b) Ethylene polymerization with Co1 – Co4/MMAO. To complement the investigation performed using MAO and explore potential co-catalysts effects,[24] **Co1** – **Co4** were also evaluated in combination with MMAO; the results of the polymerizations are compiled in Table 3.

As before, **Co1** was selected as the test precatalyst in order to determine the optimal temperature, Al/Co molar ratio and run time. With the Al/Co ratio fixed at 1000, the temperature was varied from 40 to 70 °C (runs 1-4, Table 3) with the highest activity of 4.74 × 10^6 g(PE)·mol^{-1}(Co)·h^{-1} achieved at 50 °C. Further increasing the temperature to 70 °C, the activity

gradually decreased to 2.87 × 10^6 g(PE)·mol^{-1}(Co)·h^{-1} and the molecular weight slightly decreased from 1.8 to 1.5 kg mol^{-1}. In comparison to the results observed with **Co1**/MAO, all the polyethylenes possessed much lower molecular weights across the temperature range (1.5 - 1.8 kg mol^{-1}). Furthermore, all the polymers exhibited narrower unimodal distributions (PDI < 2.0 (Co1/MMAO) *vs.* > 3.0 (Co1/MAO)) as is illustrated by their

Table 3 Ethylene polymerization results with **Co1** – **Co4** /MMAO[a]

Run	Precat.	Al/Co	T/ °C	t/min	Polymer/g	Activity[b]	M_w[c]	M_w/M_n[d]	T_m[e]/ °C
1	**Co1**	1000	40	30	5.65	3.71	1.8	2.0	121.3
2	**Co1**	1000	50	30	7.11	4.74	1.8	1.9	120.9
3	**Co1**	1000	60	30	6.30	4.20	1.5	1.7	120.5
4	**Co1**	1000	70	30	4.31	2.87	1.5	1.7	120.6
5	**Co1**	1500	50	30	7.58	5.05	1.5	1.7	120.2
6	**Co1**	2000	50	30	8.03	5.35	1.5	1.8	120.6
7	**Co1**	2250	50	30	9.29	6.19	1.4	1.7	119.6
8	**Co1**	2500	50	30	8.24	5.49	1.5	1.7	119.8
9	**Co1**	3000	50	30	5.48	3.65	1.7	1.7	119.9
10	**Co1**	2250	50	5	2.28	9.12	1.5	1.6	120.3
11	**Co1**	2250	50	15	6.15	8.20	1.5	1.7	119.7
12	**Co1**	2250	50	45	10.2	4.54	1.5	1.7	120.6
13	**Co1**	2250	50	60	10.5	3.50	1.6	1.8	120.6
14[f]	**Co1**	2250	50	30	0.52	0.35	1.2	1.7	118.8
15[g]	**Co1**	2250	50	30	4.84	3.23	1.6	1.8	120.1
16	**Co2**	2250	50	30	3.27	2.18	2.9	1.9	125.7
17	**Co3**	2250	50	30	3.94	2.63	8.2	2.2	129.8
18	**Co4**	2250	50	30	3.68	2.45	2.3	1.9	123.9

[a] Conditions: 1.5 µmol of the cobalt complex; 10 atm of ethylene; total volume of solvent 100 mL;

[b] Activity: 10^6 g(PE)·mol^{-1}(Co)·h^{-1};

[c] M_w: kg mol^{-1};

[d] M_w and M_w / M_n determined by GPC;

[e] Determined by DSC;

[f] 1 atm of ethylene;

[g] 5 atm of ethylene.

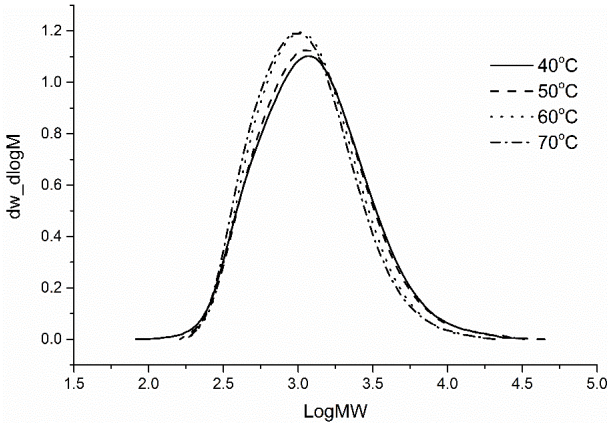

Fig. 5 GPC curves of the polymers generated using **Co1**/MMAO at different temperatures (runs 1 – 4, Table 3)

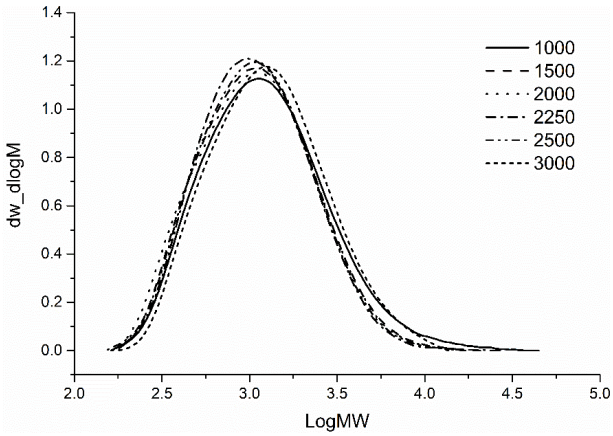

Fig. 6 GPC curves of the polyethylene obtained using **Co1**/MMAO at different Al/Co molar ratios (runs 2, 5 – 9, Table 3)

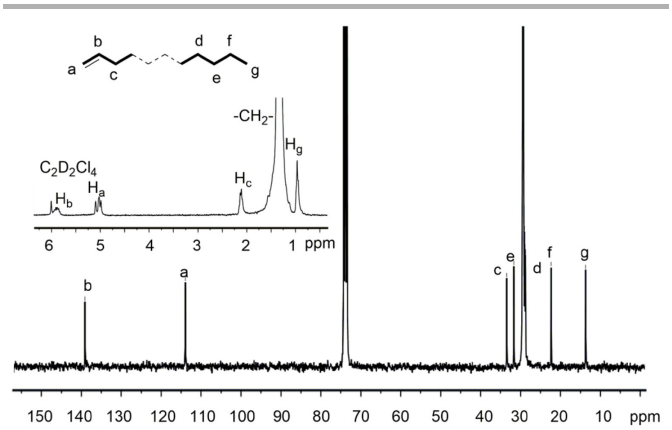

Fig. 7 ^{13}C NMR spectrum of the polyethylene obtained using **Co1**/MMAO (run 7, Table 3) (recorded in tetrachloroethane-d_2: δC 73.8 ppm), along with an insert showing its ^{1}H NMR spectrum

GPC traces (Figure 5). Indeed, these distributions are significantly narrower when compared to the very broad distributions that have previously been a characteristic of dinuclear cobalt catalysts.[6,11] The observations noted in this part of the study would suggest similar 'single-site' active species are operational at both metals without any obvious cooperative features on account of the relatively large M···M distance. As was noted with **Co1**/MAO, **Co1**/MMAO also exhibited higher activity than that seen with its mononuclear analogues;[2] a possible explanation derives from the higher net charge on cobalt by the reaction of phenol group with MAO.[25]

The influence of the Al/Co molar ratio on **Co1** was then probed by varying the ratio from 1000 to 3000 with the temperature maintained at 50 °C (runs 2, 5 - 9, Table 3). As with the results obtained using **Co1**/MAO, the highest activity of 6.19 × 10^6 g(PE)·mol^{-1}(Co)·h^{-1} was achieved at an Al/Co molar ratio of 2250; further increasing the amount of MMAO gradually decreased the level of activity. However, the molecular weight of the resultant polyethylene showed almost no change at different Al/Co molar ratios (ranging from 1.4 - 1.8 kg mol^{-1}), which may be due to limited chain transfer to aluminum.[14] Increasing the reaction time from 5 to 60 minutes gradually decreased the polymerization activity from 9.12 to 3.50 × 10^6 g(PE)·mol^{-1}(Co)·h^{-1}, while the molecular weight showed little variation; similar findings were noted using **Co1**/MAO. As mentioned earlier, decreasing the ethylene pressure significantly lowered the polymerization activity from 6.19 × 10^6 g(PE)·mol^{-1}(Co)·h^{-1} to 0.35 × 10^6 g(PE)·mol^{-1}(Co)·h^{-1} but with a minimal variation of the M_w (runs 7, 14, 15, Table 3).

Based on the optimized conditions for **Co1**/MMAO [Al/Co ratio at 2250, the temperature at 50 °C, ethylene pressure at 10 atmospheres and run time at 30 minutes], **Co2** – **Co4** were screened and their performance characteristics compared to that seen for **Co1** (runs 7, 16-18, Table 2). All cobalt species exhibited good activity (2.18 - 6.19 × 10^6 g(PE)·mol^{-1}(Co)·h^{-1}) toward ethylene polymerization but with values that are much lower than that seen with MAO. Nevertheless, the trend in activity is the same as that seen with MAO: **Co1** (Me, Me) > **Co3** (Et, Me) > **Co4** (^{i}Pr, Me) > **Co2** (Et, Et). Again the steric properties imparted by *ortho* R^1 and R^2 greatly affect the polymerization activity with the most active system **Co1** possessing the least sterically hindered environment at each metal center. In addition, all the polymers again possess narrower distributions (PDI < 2.0) and lower molecular weights than that observed with MAO as co-catalyst, the latter observation being similar to the results shown by the biphenyl-bridged bis(imino)pyridine-cobalt complexes **F**.[10]

Analysis of the high temperature ^{1}H NMR spectrum of the polymer obtained using **Co1**/MMAO (run 7, Table 3) showed resonances characteristic of a -CH=CH$_2$ group (H$_a$, H$_b$) which was confirmed in the ^{13}C NMR spectrum with the corresponding unsaturated carbon signals visible at δ 114.4 and 139.5. Unlike the polymer generated using **Co1**/MAO, the ratio of the integral for the vinylic H$_a$ (δ 5.02) to methyl H$_g$ protons (δ 0.97) in the ^{1}H NMR spectrum is slightly lower than 2:3, suggesting the coexistence of some fully saturated polyethylene. Further support for this finding comes from the ^{1}H NMR spectrum of the polymer formed in run 2 (Table 3) (shown in Figure S2), which shows an integration ratio for H$_a$/H$_g$ of 2:3.5. Furthermore, the ^{1}H NMR spectrum of the same polymer in 1,2-dichlorobenzene-d_4 reveals the ratio for H$_b$/H$_g$ to be 1:3.6, while the H$_b$:H$_a$:H$_c$ ratio remains close to the expected 1:2:2 (shown in Figure S3). The apparent presence of saturated material can be accounted for by a termination mechanism involving chain transfer to AlMe$_3$ (rather than Al(^{i}Bu$_3$)) and its derivatives present in MMAO.[14] It is unclear why with MMAO some degree of saturated polymer is also formed while with MAO uniquely vinyl-terminated materials are generated.

Conclusions

The methylene-bridged bis(imino)pyridines, L1 – L4, and their corresponding dinuclear cobalt complexes **Co1** – **Co4** have been successfully synthesized and characterized by IR spectroscopy and by elemental analysis. Furthermore, the molecular structure of **Co1** was confirmed by single crystal X-ray diffraction. On activation with MAO or MMAO, **Co1** – **Co4** displayed high activities for ethylene polymerization as well as reasonable catalytic lifetimes with the MAO-promoted systems generally resulting in polymer of higher molecular weight, while with MMAO the materials showed narrower distributions. In terms of thermal stability, **Co1**/MAO was demonstrated to be an effective catalyst at 70 °C and indeed reaching an activity greater than that observed by its most closely related mononuclear comparator. In general, highly linear polymers were formed with high levels of vinyl chain-ends. It is noteworthy that such vinyl-terminated materials are in demand for the copolymerization with ethylene to form highly branched polyethylene.

Experimental

General considerations

All manipulations involving air- and moisture-sensitive compounds were carried out under a nitrogen atmosphere using standard Schlenk techniques. Toluene was refluxed over sodium and distilled under nitrogen prior to use. Methylaluminoxane (MAO, 1.46 M solution in toluene) and modified methylaluminoxane (MMAO, 2.00 M in *n*-heptane) were purchased from Akzo Nobel Corp. High-purity ethylene was purchased from Beijing Yansan Petrochemical Co. and used as received. Other reagents were purchased from Aldrich, Acros or local suppliers. The NMR spectra of L1 – L4 were recorded on a Bruker DMX 300 or 400 MHz instrument at ambient temperature using TMS as an internal standard, while NMR spectra of the polyethylene were recorded on a Bruker DMX 300 MHz instrument at 100 °C in 1,1,2,2-tetrachloroethane-d_2 or 1,2-dichlorobenzene-d_4 as the solvent with TMS as an internal standard. IR spectra were recorded on a Perkin-Elmer System 2000 FT-IR spectrometer. Elemental analysis was carried out using a Flash EA 1112 micro-analyzer. Molecular weight and molecular weight distributions (MWD) of the polyethylene were obtained using a PL-GPC220 instrument at 150 °C using 1,2,4-trichlorobenzene as the solvent. The melting temperatures of the polyethylene were measured from the fourth scanning run on a Perkin-Elmer TA-Q2000 differential scanning calorimetry (DSC) analyzer under a nitrogen atmosphere. In the procedure, a sample of about 5.0 mg was heated to 160 °C at a rate of 20 °C min^{-1} and maintained for 2 min at 160 °C to remove the thermal history and then cooled at a rate of 20 °C min^{-1} to 20 °C. Compounds $CH(C_6H_4\text{-}4\text{-}OH)(4\text{-}C_6H_2\text{-}2,6\text{-}R_2NH_2)_2$ (R = Me, Et) and 2-(CMeO)-6-{(CMe=N(2,6-$R^1{}_2C_6H_3$)}C_5H_3N (R^1 = Me, Et, ^{i}Pr) were prepared according to literature procedures.[13]

4-(Bis(4-((1-(6-(1-((2,6-dimethylphenyl)imino)ethyl)pyridin-2-yl)ethylidene)amino)-3,5-dimethylphenyl)methyl)phenol (L1)

A catalytic amount of *p*-toluenesulfonic acid was added to a solution of 2-(CMeO)-6-{(CMe=N(2,6-$Me_2C_6H_3$)}C_5H_3N (2.61 g, 10.0 mmol) and $CH(C_6H_4\text{-}4\text{-}OH)(4\text{-}C_6H_2\text{-}2,6\text{-}Me_2NH_2)_2$ (1.40 g, 4.0 mmol) in *o*-xylene (150 mL) and the resulting mixture stirred and heated to reflux for 12 h. On cooling to room temperature, the solvent was removed by rotary evaporation and the residue purified by column chromatography with petroleum ether/ethyl acetate (12 : 1) and a few drops of triethylamine as eluent affording L1 as a yellow solid (0.58 g, 17%). ^{1}H NMR (300 MHz, $CDCl_3$): δ 8.48 (d, *J* = 7.5 Hz, 4H, Py-*H*), 7.92 (t, *J* = 7.8 Hz, 2H, Py-*H*), 7.08 (d, *J* = 7.5 Hz, 4H, Ar-*H*), 6.97 (t, *J* = 6.9 Hz, 4H, Ar-*H* and Ph-*H*), 6.87 (d, *J* = 6.9 Hz, 4H, Ar-*H*), 6.60 (d, *J* = 7.8 Hz, 2H, Ph-*H*), 5.37 (s, 1H, $(Ar)_2$-C*H*-Ph), 2.26 (d, *J* = 12.0 Hz, 12H, -CH_3), 2.03 (t, *J* = 7.2 Hz, 24H, -CH_3). ^{13}C NMR (75 MHz, $CDCl_3$): δ 168.3, 167.4, 155.1, 154.4, 148.8, 146.5, 139.7, 137.6, 137.1, 136.8, 130.6, 129.3, 129.2, 128.1, 125.6, 125.5, 125.4, 123.2, 122.5, 115.2, 55.2, 18.3, 18.1, 17.0, 16.6. FT-IR (KBr, cm^{-1}): 2919 (m), 2854 (w), 1641 (s, $\nu_{C=N}$), 1571 (m), 1510 (m), 1469 (s), 1362 (s), 1323 (w), 1296 (w), 1251 (m), 1206 (s), 1170 (w), 1145 (w), 1120 (s), 1096 (m), 1026 (w), 965 (w), 881 (w), 816 (s), 767 (s),739 (w), 692 (w), 667 (w), 606 (w), 530 (w), 402 (w). Anal. Calcd. for $C_{57}H_{58}N_6O$ (842.47): C, 81.20; H, 6.93; N, 9.97%. Found: C, 81.59; H, 7.27; N, 10.10%.

4-(Bis(4-((1-(6-(1-((2,6-diethylphenyl)imino)ethyl)pyridin-2-yl)ethylidene)amino)-3,5-diethylphenyl)methyl)phenol (L2)

Using the same procedure and chromatographic work-up as described for the synthesis of L1, L2 was isolated as a yellow solid (0.21 g, 22%). ^{1}H NMR (300 MHz, $CDCl_3$): δ 8.39 (d, *J* = 8.1Hz, 4H, Py-*H*), 7.81 (t, *J* = 7.8 Hz, 2H, Py-*H*), 7.02 (d, *J* = 6.9 Hz, 4H, Ar-*H*); 6.95 (d, *J* = 6.3 Hz, 2H, Ar-*H*), 6.91 (d, *J* = 7.5 Hz, 2H, Ph-*H*), 6.85 (s, 2H, Ar-*H*), 6.81 (s, 2H, Ar-*H*), 6.50 (d, *J* = 8.7 Hz, 2H, Ph-*H*), 5.35 (s, 1H, $(Ar)_2$-C*H*-Ph), 2.38-2.24 (m, 16H, -CH_2CH$_3$), 2.20 (s, 6H, -CH_3), 2.17 (s, 6H, -CH_3), 1.08-0.95 (m, 24H, -CH_3). ^{13}C NMR (75 MHz, $CDCl_3$): δ 167.0, 166.1, 154.2, 154.1, 153.5, 146.8, 144.4, 139.0, 136.1, 135.8, 130.3, 130.2, 130.1, 129.4, 126.4, 126.3, 125.0, 122.5, 121.4, 114.2, 54.6, 35.7, 30.7, 23.7, 16.2, 15.9, 13.0, 12.8. FT-IR (KBr, cm^{-1}): 2963 (m), 2928 (m), 2870 (w), 1640 (s, $\nu_{C=N}$), 1570 (w), 1510 (w), 1453 (s), 1364 (s), 1323 (w), 1296 (w), 1256 (s), 1201 (m), 1170 (w), 1143 (w), 1100 (s), 1078 (s), 1020 (m), 967 (w), 877 (w), 801 (s), 767 (s), 740 (w), 669 (w), 630 (w), 529 (w). Anal. Calcd. for $C_{65}H_{74}N_6O$ (954.59): C, 81.72; H, 7.81; N, 8.80%. Found: C, 81.86; H, 8.11; N, 8.63%.

4-(Bis(4-((1-(6-(1-((2,6-diethylphenyl)imino)ethyl)pyridin-2-yl)ethylidene)amino)-3,5-dimethylphenyl)methyl)phenol (L3)

Using the same procedure and chromatographic work-up as described for the synthesis of L1, L3 was isolated as a yellow solid (0.68 g, 19%). ^{1}H NMR (400 MHz, $CDCl_3$): δ 8.48 (d, *J* = 7.6 Hz, 4H, Py-*H*), 7.91 (t, *J* = 8.0 Hz, 2H, Py-*H*), 7.12 (d, *J* = 7.6 Hz, 4H, Ar-*H*), 7.06-6.98 (m, 4H, Ar-*H* and Ph-*H*), 6.87 (d, *J* = 5.6 Hz, 4H, Ar-*H*), 6.62 (d, *J* = 7.6 Hz, 2H, Ph-*H*), 5.37 (s, 1H, $(Ar)_2$-C*H*-Ph), 2.48-2.31 (m, 8H, -CH_2CH$_3$), 2.27 (d, *J* = 10.4 Hz, 12H, -CH_3), 2.03 (s, 12H, -CH_3), 1.15 (t, *J* = 7.6 Hz, 12H, -CH_3). ^{13}C NMR (100 MHz, $CDCl_3$): δ 168.1, 167.1, 155.4, 155.3, 154.6, 147.9, 146.6, 139.7, 137.1, 136.7, 131.4, 130.6, 129.3, 129.2, 126.1, 125.5, 123.5, 122.4, 115.3, 55.3, 46.1, 54.0, 27.1, 24.8, 18.3, 17.0, 16.9, 13.9, 11.1. FT-IR (KBr, cm^{-1}): 2964 (w), 2929 (w), 2870 (w), 1641 (s, $\nu_{C=N}$), 1571 (w), 1450 (s), 1363 (s), 1323 (w), 1295 (w), 1243 (m), 1207 (s), 1170 (w), 1144 (w), 1119 (m), 1101 (m), 1076 (w), 1029 (w), 964 (w), 876 (w), 818 (s), 768 (s), 73 7(m), 667 (w), 633 (w), 607 (w), 529 (w). Anal. Calcd. for $C_{61}H_{66}N_6O$ (898.53): C, 81.48; H, 7.40; N, 9.35%. Found: C, 81.11; H, 7.76; N, 9.74%.

4-(Bis(4-((1-(6-(1-((2,6-diisopropylphenyl)imino)ethyl)pyridin-2-yl)ethylidene)amino)-3,5-dimethylphenyl)methyl)phenol (L4)

Using the same procedure and chromatographic work-up as described for the synthesis of L1, L4 was isolated as a yellow solid (1.30 g, 33%). ^{1}H NMR (300 MHz, $CDCl_3$): δ 8.40 (d, *J* = 7.8 Hz, 4H, Py-*H*), 7.84 (t, *J* = 7.8 Hz, 2H, Py-*H*), 7.09 (d, *J* = 6.6 Hz, 4H, Ar-*H*), 7.03 (t, *J* = 4.5 Hz, 2H, Ar-*H*), 6.90 (d, *J* = 8.4 Hz, 2H, Ph-*H*), 6.79 (d, *J* = 7.5 Hz, 4H, Ar-*H*), 6.51 (d, *J* = 8.7 Hz, 2H, Ph-*H*), 5.29 (s, 1H$(Ar)_2$-C*H*-Ph), 2.73-2.64 (m, 4H, -C*H*$(CH_3)_2$), 2.20(d, *J* = 4.8 Hz, 12H, -CH_3), 1.95 (d, *J* = 6.0 Hz, 12H, -CH_3), 1.08 (d, *J* = 6.9 Hz, 24H, -CH_3). ^{13}C NMR (75 MHz, $CDCl_3$): δ 167.3, 165.9, 154.1, 153.9, 153.3, 145.4, 145.3, 138.5, 135.9, 135.6, 134.8, 129.4, 128.1, 128.0, 124.4, 122.6, 122.0, 121.3, 114.0, 63.4, 59.4, 54.0, 27.3, 22.2, 21.9, 17.1, 16.2, 15.9. FT-IR (KBr, cm^{-1}): 2960 (m), 2925 (w), 2868 (w), 1640 (s, $\nu_{C=N}$), 1572 (w), 1512 (m), 1453 (m), 1363 (s), 1323 (w), 1299 (w), 1237

(m), 1212 (s), 1171 (w), 1146 (w), 1119 (m), 1078 (w), 1040 (w), 996 (w), 964 (w), 936 (w), 881 (w), 820 (m), 797 (w), 769 (s), 739 (w), 705 (w), 635 (w), 607 (w), 528 (w), 419 (w). Anal. Calcd. for $C_{65}H_{74}N_6O$ (954.59): C, 81.72; H, 7.81; N, 8.80%. Found: C, 81.98; H, 8.19; N, 9.19%.

Preparation of Co1 – Co4

Co1. L1 (0.17 g, 0.2 mmol) and $CoCl_2$ (0.052 g, 0.4 mmol) were added to a Schlenk tube followed by freshly distilled dichloromethane (10 mL) and the mixture stirred at room temperature overnight. The resulting precipitate was filtered, washed with diethyl ether and dried under reduced pressure to give **Co1** as a yellow powder (0.14 g, 72%). FT-IR (KBr, cm^{-1}): 3383 (w), 2963 (m), 2923 (m), 2868 (w), 1618 (w, $\nu_{C=N}$), 1586 (s), 1511 (w), 1468 (m), 1440 (m), 1370 (s), 1321 (w), 1261 (s), 1216 (s), 1175 (w), 1099 (m), 1031 (m), 881 (w), 800 (s), 773 (w), 745 (w), 672 (w), 527 (w), 442 (w), 419 (w). Anal. Calcd. for $C_{57}H_{58}Cl_4Co_2N_6O{\cdot}2H_2O$ (1136.23): C, 60.12; H, 5.49; N, 7.38%. Found: C, 60.22; H, 5.40; N, 7.19%.

Co2. Using the same procedure and molar ratios as described for the synthesis of **Co1**, **Co2** was obtained as a yellow powder (0.15 g, 69%). FT-IR (KBr, cm^{-1}): 3380 (w), 2963 (m), 2923 (m), 2868 (w), 1617 (w, $\nu_{C=N}$), 1586 (s), 1511 (w), 1466 (m), 1440 (m), 1370 (s), 1321 (w), 1261 (s), 1215 (s), 1175 (w), 1099 (m), 1030 (m), 881 (w), 800 (s), 772 (w), 744 (w), 672 (w), 642 (w), 610 (w), 527 (w), 466 (w), 439 (w). Anal. Calcd. for $C_{65}H_{74}Cl_4Co_2N_6O{\cdot}2H_2O$ (1248.36): C, 62.41; H, 6.28; N, 6.72%. Found: C, 62.43; H, 5.91; N, 6.48%.

Co3. Using the same procedure and molar ratios as described for the synthesis of **Co1**, **Co3** was obtained as a yellow powder (0.18 g, 87%). FT-IR (KBr, cm^{-1}): 3207 (w), 2963 (m), 2930 (w), 2875 (w), 1621 (m, $\nu_{C=N}$), 1587 (s), 1511 (m), 1472 (m), 1443 (m), 1370 (s), 1320 (w), 1262 (s), 1216 (s), 1175 (w), 1105 (w), 1027 (w), 853 (w), 808 (s), 775 (w), 746 (w), 672 (w), 642 (w), 611 (w), 575 (w), 528 (w). Anal. Calcd. for $C_{61}H_{66}Cl_4Co_2N_6O{\cdot}2H_2O$ (1192.29): C, 61.31; H, 5.90; N, 7.03%. Found: C, 61.64; H, 5.69; N, 7.04%.

Co4. Using the same procedure and molar ratios as described for the synthesis of **Co1**, **Co4** was obtained as a yellow powder (0.19 g, 87%). FT-IR (KBr, cm^{-1}): 3388 (w), 2962 (m), 2923 (w), 2868 (w), 1618 (w, $\nu_{C=N}$), 1587 (s), 1511 (w), 1468 (m), 1441 (m), 1371 (s), 1320 (w), 1260 (s), 1216 (s), 1175 (w), 1101 (m), 1029 (m), 937 (w), 881 (w), 800 (s), 774 (w), 743 (w), 672 (w), 643 (w), 607 (w), 525 (w), 466 (w), 441 (w). Anal. Calcd. for $C_{65}H_{74}Cl_4Co_2N_6O{\cdot}2H_2O$ (1248.36): C, 62.41; H, 6.28; N, 6.72%. Found: C, 62.75; H, 5.95; N, 6.36%.

Ethylene polymerization at 5/10 atm ethylene pressure

The polymerization at 5 or 10 atm of ethylene pressure was carried out in a 250 mL stainless steel autoclave equipped with a mechanical stirrer and temperature controller. The autoclave was evacuated and refilled with nitrogen two times and then with ethylene one time. When the required temperature was reached, the pre-catalyst (1.5 μmol) dissolved in toluene (25 mL) was injected into the autoclave under an ethylene atmosphere (~ 1 atm), followed by the addition of more toluene (50 mL). The required amount of co-catalyst (MAO, MMAO) and additional toluene were added successively by syringe taking the total volume of toluene to 100 mL. The autoclave was immediately pressurized with 5/10 atm. pressure of ethylene and the stirring commenced. After the required reaction time, the reactor was cooled with a water bath and the excess ethylene vented. The reaction was then quenched with 10% hydrochloric acid in ethanol and the precipitated polymer collected, washed with ethanol and then dried under reduced pressure at 50 °C and weighed.

Ethylene polymerization at 1 atm ethylene pressure. The polymerization at 1 atm ethylene pressure was carried out in a Schlenk tube. Under an ethylene atmosphere (1 atm), **Co1** (1.5 μmol) was added followed by toluene (30 mL) and then the required amount of co-catalyst (MAO, MMAO) introduced by syringe. The resulting solution was stirred at the required temperature under 1 atm of ethylene. After 30 min, the solution was quenched with 10% hydrochloric acid in ethanol. The polymer was washed with ethanol, dried under reduced pressure at 40 °C and then weighed.

X-ray structure determination

Table 4. Crystal data and structure refinement details for **Co1**

Empirical formula	$C_{57}H_{58}Cl_4Co_2N_6O$
Formula weight	1102.76
Temperature/K	173.15
Wavelength/Å	0.71073
Crystal system	monoclinic
Space group	C2/c
a/Å	15.2036(5)
b/Å	24.5959(6)
c/Å	34.1168(11)
Alpha/°	90
Beta/°	94.102(3)
Gamma/°	90
Volume/Å^3	12725.2(7)
Z	8
Dcalcd /(g cm^{-3})	1.151
μ/mm^{-1}	0.728
F(000)	4576.0
Crystal size/mm^3	0.123 × 0.043 × 0.032
θ range/°	3.156 - 63.256
Limiting indices	-21 ≤ h ≤ 21
	-33 ≤ k ≤ 35
	-49 ≤ l ≤ 47
No. of rflns collected	85709
No. unique rflns	19779
R(int)	0.1344
No. of params	644
Completeness to θ	0.924
Goodness of fit on F^2	1.022
Final R indices [I ≥ 2σ(I)]	R_1 = 0.0938
	wR_2 = 0.2161
R indices (all data)	R_1 = 0.2230
	wR_2 = 0.2755
Largest diff. peak and hole/(e Å^{-3})	0.54/-0.29

A single-crystal X-ray diffraction study of **Co1** was conducted on a Rigaku Sealed Tube CCD (Saturn 724+) diffractometer

with graphite-monochromated Mo-Kα radiation (λ = 0.71073 Å) at 173(2) K; the cell parameters were obtained by global refinement of the positions of all collected reflections. Intensities were corrected for Lorentz and polarization effects and empirical absorption. The structures were solved by direct methods and refined by full-matrix least-squares on F^2. All non-hydrogen atoms were refined anisotropically and all hydrogen atoms were placed in calculated positions. Structure solution and structure refinement were performed by using the SHELXT (Sheldrick, 2015).[26] Crystal data and processing parameters for **Co1** are summarized in Table 4.

Conflicts of interest

There are no conflicts to declare.

Acknowledgements

This work was supported by the National Natural Science Foundation of China (Nos. 51473170, and U1362204). GAS thanks the Chinese Academy of Sciences for a Visiting Fellowship.

Notes and references

1 (a) L. K. Johnson, C. M. Killian, and M. Brookhart, *J. Am. Chem. Soc.*, 1995, **117**, 6414; (b) C. M. Killian, D. J. Tempel, L. K. Johnson and M. Brookhart, *J. Am. Chem. Soc.*, 1996, **118**, 11664.

2 (a) B. L. Small, M. Brookhart and A. M. A. Bennett, *J. Am. Chem. Soc.*, 1998, **120**, 4049; (b) G. J. P. Britovsek, V. C. Gibson, B. S. Kimberley, P. J. Maddox, S. J. McTavish, G. A. Solan, A. J. P. White and D. J. Williams, *Chem. Commun.*, 1998, 849; (c) E. Yue, Y. Zeng, W. Zhang, Y. Sun, X.-P. Cao, W.-H. Sun, *Sci China Chem*., 2016, **59**, 1291; (d) Z. Wang, G. A. Solan, Q. Mahmood, Q. Liu, Y. Ma, X. Hao, W.-H. Sun, *Organometallics*, 2018, **37**, 380; (e) Q. Mahmood, J. Guo, W. Zhang, Y. Ma, T. Liang, W.-H. Sun, *Organometallics*, 2018, **37**, 957.

3 A. L. Gavrilova and B. Bosnich, *Chem. Rev*. 2004, **104**, 349.

4 M. Delferro and T. J. Marks, *Chem. Rev*. 2011, **111**, 2450.

5 (a) Q. Khamker, Y. D. M. Champouret, K. Singh and G. A. Solan, *Dalton Trans*., 2009, **41**, 8935; (b) A.P. Armitage, Y. D. M. Champouret, H. Grigoli, J. D. A. Pelletier, K. Singh, and G. A. Solan, *Eur. J. Inorg. Chem.*, 2008, **29**, 4597.

6 C. Bianchini, G. Giambastiani, I. Guerrero Rios, A. Meli, W. Oberhauser, L. Sorace, and A. Toti, *Organometallics*, 2007, **26**, 5066.

7 W.-H. Sun, Q. Xing, J. Yu, E. Novikova, W. Zhao, X. Tang, T. Liang, and C. Redshaw, *Organometallics*, 2013, **32**, 2309.

8 S. Zhang, I. Vystorop, Z. Tang, and W.-H. Sun, *Organometallics*, 2007, **26**, 2456.

9 P. Barbaro, C. Bianchini, G. Giambastiani, I. G. Rios, A. Meli, W.Oberhauser, A. M. Segarra, L. Sorace, and A. Toti, *Organometallics*, 2007, **26**, 4639.

10 Q. Xing, T. Zhao, S. Du, W. Yang, T. Liang, C. Redshaw, and W.-H. Sun, *Organometallics*, 2014, **33**, 1382.

11 D. Takeuchi, S. Takano, Y. Takeuchi, and K. Osakada, *Organometallics*, 2014, **33**, 5316.

12 (a) V. C. Gibson, C. Redshaw, and G. A. Solan, *Chem. Rev*., 2007, **107**, 1745; (b) J. Ma, C. Feng, S. Wang, K-Q. Zhao, W.-H. Sun, C. Redshaw and G. A. Solan, *Inorg. Chem. Front*., 2014, **1**, 14; (c) J. Wang, W. Li, B. Jiang, Y. Yang, *J. Appl Polym. Sci.*, 2009, **113**, 2378.

13 (a) G. A. Solan, J. D. A. Pelletier, WO2005/118605(A1), December 15, 2005; (b) C. Bianchini, G. Mantovani, A. Meli, F. Migliacci, F. Zanobini, F. Laschi, and A. Sommazzi, *Eur. J. Inorg. Chem*. 2003, **8**, 1620.

14 G. J. P. Britovsek, M. Bruce, V. C. Gibson, B. S. Kimberley, P. J. Maddox, S. Mastroianni, S. J. McTavish, C. Redshaw, G. A. Solan, S. Stromberg, A. J. P. White, and D. J. Williams, *J. Am. Chem. Soc.* 1999, **121**, 8728.

15 (a) J. Yu, W. Huang, L. Wang, C. Redshaw and W.-H. Sun, *Dalton Trans*., 2011, **40**, 10209; (b) S. Wang, B. Li, T. Liang, C. Redshaw, Y. Li. W.-H. Sun, *Dalton Trans.*, 2013, **42**, 9188; (c) W. Zhang, S. Wang, S. Du, C.-Y. Guo, X. Hao, W.-H. Sun, *Macromol. Chem. Phys*. 2014, **215**, 1797; (d) N. E. Mitchell, W. C. Anderson, Jr., B. K. Long, *J. Polym. Sci., part A: polym. Chem.*, 2017, **55**, 3990.

16 (a) S. A. Svejda and M. Brookhart, *Organometallics*, 1999**,** **18**, 65; (b) A. K. Tomov, V. C. Gibson, G. J. P. Britovsek, R. J. Long, M. van Meurs, D. J. Jones, K. P. Tellmann, and J. J. Chirinos, *Organometallics*, 2009, **28**, 7033.

17 (a) S. Wang, B. Li, T. Liang, C. Redshaw, Y. Li and W.-H. Sun, *Dalton Trans*., 2013, **42**, 9188; (b) J. Ba, S. Du, E. Yue, X. Hu, Z. Flisak and W.-H. Sun, *RSC Adv.*, 2015, **5**, 32720.

18 T. Xiao, P. Hao, G. Kehr, X. Hao, G. Erker and W.-H. Sun, *Organometallics*, 2011, **30**, 4847.

19 N.V. Semikolenova, V.A. Zakharov, L.G. Echevskaja, M.A. Matsko, K.P. Bryliakov, E.P. Talsi, *Catalysis Today*, 2009, **144**, 334.

20 F. Huang, W. Zhang, E. Yue, T. Liang, X. Hu, W. -H. Sun. *Dalton Trans*., 2016, **45**, 657.

21 J. Yu, H. Liu, W. Zhang, X. Hao and W.-H. Sun, *Chem. Commun*., 2011, **47**, 3257.

22 G. B. Galland, R. Quijada, R. Rojas, G. Bazan, Z. J. A. Komon, *Macromolecules*, 2002, **35**, 339.

23 (a) F. Huang, W. Zhang, Y. Sun, X. Hu, G. A. Solan, W.-H. Sun, *New J. Chem*., 2016, **40**, 8012; (b) C. Huang, Y. Zhang, G. A. Solan, Y. Ma, X. Hu, Y. Sun, and W.-H. Sun, *Eur. J. Inorg. Chem*. 2017, **36**, 4158.

24 (a) B. K. Bahuleyan, G. W. Son, D-W. Park, C-S. Ha, I. Kim, *J. Polym. Sci.: Part A: Polym. Chem.*, 2008. **46**, 1066; (b) S. A. Svejda, M. Brookhart, *Organometallics*, 1999, **18**, 65; (c) E.Y-X. Chen, T. J. Marks, *Chem. Rev*. 2000, **100**, 1391.

25 (a) T. Zhang, D. Guo, S. Jie, W-H. Sun, T. Li, X. Yang, *J. Polym. Sci., Part A: Polym. Chem*., 2004, **42**, 4765; (b) W. Yang, J. Yi, W-H. Sun, *Macromol. Chem. Phys*. 2015, **216**, 1125.

26 (a) G. M. Sheldrick, *Acta Crystallogr., Sect A: Found. Adv.* 2015, **71**, 3-8; (b) G. M. Sheldrick, *Acta Crystallogr., Sect C: Struct. Chem.* 2015, **71**, 3-8.